Adsorption of Methylene Blue Dye onto Carbon Nanotubes: A Route to an Electrochemically Functional Nanostructure and Its Layer-by-Layer Assembled Nanocomposite

Yiming Yan,† Meining Zhang,† Kuanping Gong,† Lei Su, Zhixin Guo, and Lanqun Mao*

Center for Molecular Science, Institute of Chemistry, Chinese Academy of Sciences, Beijing 100080, China

Received February 23, 2005. Revised Manuscript Received May 3, 2005

This paper describes the adsorption of electroactive methylene blue (MB) dye onto single-walled carbon nanotubes (SWNTs) to form an electrochemically functional nanostructure and its layered nanocomposite. UV−visible and FT-IR spectroscopy and electrochemistry used for characterization of the MB adsorption onto SWNTs reveal that MB essentially interacts with SWNTs through charge-transfer and hydrophobic interactions, leading to the formation of a MB−SWNT adsorptive nanostructure which exhibits distinct electrochemical properties from those of MB adsorbed onto a glassy carbon (GC) electrode. The interactions between MB and the SWNTs are demonstrated to closely associate with the structural properties of the SWNTs by comparing the electrochemical properties of MB adsorbed onto different substrates, i.e., glassy carbon, SWNTs, and SWNTs intentionally sidewall functionalized with hydroxyl groups (SWNT-OHs). The stable adsorption of water-soluble and positively charged MB molecules onto the SWNTs is further demonstrated to be able to solubilize the formed nanostructure in water quite well and to fabricate a functional nanocomposite by layer-by-layer assembling of the formed nanostructure on a solid substrate.

Introduction

Considerable attention has been drawn to the carbon nanotubes (CNTs) over the past decade because of their unique physical and chemical properties and potential applications in various research and industrial fields.[1] Attempts to date have witnessed successes in the preparation of the CNTs and understanding of their chemical and physical properties.[2] In recent years, increasing interests are being focused on the rational functionalization of the CNTs to fabricate functional nanostructures with novel properties and some creative methods have been used for the functionalization of the CNTs, e.g., with biomolecules and metal nanoparticles, through a covalent or noncovalent interaction.[3] To this end, these functionalization strategies have generated a large variety of new nanostructures with excellent functions which are very attractive for practical applications.[4] For example, the noncovalent adsorption of biomolecules, such as enzyme and proteins, onto the sidewalls of the CNTs has resulted in novel CNT-based nanostructures consisting of biorecognition units, offering an efficient route to bioelectronic nanodevices, e.g., biosensors and bioelectronics.[5] In addition to the efforts on the construction of functional nanostructures, recent attempts have also been made to fabricate CNT-based nanocomposites, which is another key issue relevant to functional nanodevices.[6] In particular, methods such as sol−gel and layer-by-layer assembly have been used for integrating the CNT nanostructures into nanocomposites as nanodevices for practical applications.[7]

We demonstrate here a new type of electrochemically functional nanostructure and its layered nanocomposite through the adsorption of electroactive methylene blue (MB) onto single-walled carbon nanotubes (SWNTs). It is known that the π-stacking interaction between the aromatic compounds, e.g., MB, and flat graphite essentially results in a stable adsorption of such kind of compounds on the graphitic

* Corresponding author. Fax: +86-10-62559373. E-mail: lqmao@iccas.ac.cn.
† Also in Graduate School of the CAS.

(1) (a) Ajayan, P. M. *Chem. Rev.* **1999**, *99*, 1787. (b) Baughman, R. H.; Zakhidov, A. A.; de Heer, W. A. *Science* **2002**, *297*, 787. (c) Sun, Y.; Fu, K.; Lin, Y.; Huang, W. *Acc. Chem. Res.* **2002**, *35*, 1096. (d) Dai, L.; Soundarrajan, P.; Kim, T. *Pure Appl. Chem.* **2002**, *74*, 1753.

(2) (a) Andrews, R.; Jacques, D.; Qian, D.; Rantell, T. *Acc. Chem. Res.* **2002**, *35*, 1008. (b) Wong, E. W.; Sheehan, P. E.; Lieber, C. M. *Science* **1997**, *277*, 1971.

(3) (a) Guldi, D. M.; Marcaccio, M.; Paolucci, D.; Paolucci, F.; Tagmatarchis, N.; Tasis, D.; Vázquez, E.; Prato, M. *Angew. Chem., Int. Ed.* **2003**, *42*, 4206. (b) Ellis, A. V.; Vijayamohanan, K.; Goswami, R.; Chakrapani, N.; Ramanathan, L. S.; Ajayan, P. M.; Ramanath, G. *Nano Lett.* **2003**, *3*, 279. (c) Dieckmann, G. R.; Dalton, A. B.; Johnson, P. A.; Razal, J.; Chen, J.; Giordano, G. M. *J. Am. Chem. Soc.* **2003**, *125*, 1770. (d) Azamian, B. R.; Davis, J. J. *J. Am. Chem. Soc.* **2002**, *124*, 12664. (e) Haremza, J. M.; Kahn, M. A. *Nano Lett.* **2002**, *2*, 1253. (f) Li, H.; Zhou, B.; Lin, Y.; Gu, L.; Wang, W.; Fernando, K. A. S.; Kumar, S.; Allard, L. F.; Sun, Y. *J. Am. Chem. Soc.* **2004**, *126*, 1014.

(4) (a) Dai, H. *Acc. Chem. Res.* **2002**, *35*, 1035−1044. (b) Star, A.; Stoddart, J.; Steuerman, D.; Diehl, M.; Boukai, A. *Angew. Chem., Int. Ed.* **2001**, *40*, 1721.

(5) Chen, R. J.; Zhang, Y.; Wang, D.; Dai, H. *J. Am. Chem. Soc.* **2001**, *123*, 3838.

(6) (a) Lou, X.; Detrembleur, C.; Pagnoulle, C.; Jérôme, R.; Bocharova, V.; Kiriy, A.; Stamm, M. *Adv. Mater.* **2004**, *16*, 2123. (b) Shimoda, H.; Oh, S. J.; Geng, H. Z.; Walker, R. J.; Zhang, X. B.; McNeil, L. E.; Zhou, O. *Adv. Mater.* **2002**, *14*, 899. (c) Rouse, J. H.; Lillehei, P. T.; Sanderson, J.; Siochi, E. J. *Chem. Mater.* **2004**, *16*, 3904. (d) Zhu, J.; Yudasaka, M.; Zhang, M.; Kasuya, D.; Iijima, S. *Nano Lett.* **2003**, *3*, 1239.

(7) (a) Zhang, M.; Gong, K.; Zhang, H.; Mao, L. *Biosens. Bioelectron.* **2005**, *7*, 1270. (b) Gong, K.; Zhang, M.; Yan, Y.; Su, L.; Mao, L.; Xiong, S.; Chen, Y. *Anal. Chem.* **2004**, *76*, 6500. (c) Zhang, M.; Yan, Y.; Gong, K.; Mao, L.; Guo, Z.; Chen, Y. *Langmuir* **2004**, *20*, 8781. (d) Rouse, J. H.; Lillehei, P. T. *Nano Lett.* **2003**, *3*, 59. (e) Kovtyuhova, N. I.; Mallouk, T. E. *Adv. Mater.* **2005**, *17*, 187. (f) Qin, S.; Qin, D.; Ford, W. T.; Herrera, J. E.; Resasco, D. E. *Macromolecules* **2004**, *37*, 9963.

10.1021/cm0504182 CCC: $30.25
Published on Web 05/27/2005

Scheme 1. Chemical Structure of Methylene Blue

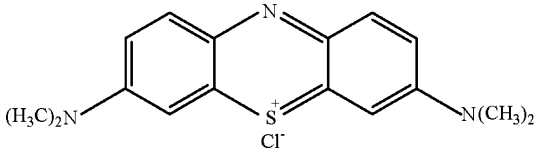

surface.[8] Compared with the flat graphite, the CNTs consist of seamlessly rolled-up graphene sheets of carbon, exhibiting a special sidewall curvature and possessing a π-conjugative structure with a highly hydrophobic surface. These unique properties of the CNTs essentially allow them to interact with some organic compounds, (polynuclear) aromatic compounds, in particular, through $\pi-\pi$ electronic and hydrophobic interactions and thus form new nanostructures as demonstrated previously.[9] The present choice of MB to noncovalently functionalize the SWNTs and fabricate a new type of electrochemically functional nanostructure is because, as one kind of polynuclear aromatic electroactive dyes, MB can be expected to strongly interact with the SWNTs to form a new kind of stable MB-SWNT nanostructure. More importantly, MB possesses good electrochemical properties and has been widely used for basic electrochemical studies and applications, for example, electrocatalysis, solar cells, and biosensors.[10] Therefore, the prepared functional MB−SWNT nanocomposite is reasonably envisaged to be very useful for development of novel electronic nanodevices, e.g., biosensors and photovoltaic cells. Furthermore, as demonstrated in the text, the adsorption of MB onto the SWNTs is found not only to solubilize the formed MB−SWNT nanostructure in water quite well but also to facilitate layer-by-layer assembling of the prepared electrochemically functional nanostructure into a nanocomposite. To the best of our knowledge, the present strategy for the preparation of an electrochemically functional nanostructure and its nanocomposite through the adsorption of electroactive moieties onto the SWNTs and layer-by-layer method has not been reported so far. The prepared MB−SWNT nanocomposite is believed to be very useful for electrochemical studies and as a new type of electronic nanodevice for practical applications.

Experimental Section

Chemicals and Materials. Poly(diallyldimethylammonium chloride) (PDDA, $M_w = 200000-350000$, 20% aqueous solution) and polystyrene sulfonate (PSS, $M_w = 70000$) were obtained from Aldrich and used as received. Methylene blue (MB, structure shown in Scheme 1) was purchased from Beijing Chemical Company (Beijing, China). Single-walled carbon nanotubes (SWNTs, with an average diameter of about 20 nm) were purchased from Nanoport Co. Ltd. (Shenzhen, China). The SWNTs were purified by refluxing the as-received SWNTs in 2.6 M HNO_3 for 10 h.

The sidewall functionalization of the SWNTs with hydroxyl groups was carried out based on a solid-state mechanochemical reaction as reported previously.[11] Briefly, the SWNTs (10 mg) and potassium hydroxide (200 mg) were weighed into a stainless steel capsule containing a milling ball. Then, the capsule was vigorously shaken for 2 h at room temperature. The reaction mixture was dissolved in 10 mL of distilled water and repeatedly precipitated into methanol to ensure a complete removal of potassium hydroxide residue. The obtained SWNTs functionalized with multiple hydroxyl groups (SWNT-OHs) were hydrophilic and can be dispersed in distilled water and ethanol. Other chemicals were of analytical grade or higher and used without further purification. Aqueous solutions were prepared with doubly distilled water.

Characterization of MB Adsorption onto SWNTs. MB adsorption onto the SWNTs was characterized with UV−vis and FT-IR spectroscopy and electrochemistry. The MB−SWNT adsorptive nanostructure used for the characterization (and layer-by-layer assembling, as detailed later) was prepared by sonicating a mixture consisting of 2 mg of the SWNTs and 5 mg of MB in 10 mL of distilled water for 2 h at room temperature. The resulting suspension was filtered with a Millipore porous filter (0.45 μm, Millipore). The obtained sample was first thoroughly rinsed with distilled water to remove nonadsorbed MB and then dried at 75 °C for 5 h to obtain the MB−SWNT adduct. The adduct was dispersed in distilled water for UV−vis spectroscopic measurements performed with a UV−visible spectrophotometer (UV-1601PC, Shimadzu, Japan), pressed into a KBr pellet for FT-IR measurements with Tensor 27 Infrared Spectrometer (Bruker, Germany), and confined onto a glassy carbon (GC) electrode for electrochemical measurements.

For electrochemical measurements, the GC electrodes were first polished with emery paper (# 2000), 0.3 and 0.05 μm alumina slurry on a woolen cloth, then cleaned under bath sonication for 10 min, and finally thoroughly rinsed with distilled water. For confining the MB−SWNT nanostructure onto a GC electrode, the prepared MB−SWNT was dispersed into water and 4 μL of the homogeneous suspension was coated onto the GC electrodes. The electrode (denoted as MB−SWNT/GC, hereafter) was then dried to evaporate the solvent. Alternatively, the MB−SWNT/GC electrode could also be prepared by immersing the SWNT/GC electrode into phosphate buffer (pH 7.0) containing 1.0×10^{-4} M MB for 3 h. The SWNT/GC electrode was prepared by coating 4 μL of SWNT dispersion in DMF (1 mg/mL) onto GC electrode. The as-prepared MB−SWNT/GC electrode was thoroughly rinsed with water to remove the nonadsorbed MB. For comparison, SWNT-OH/GC electrodes were prepared with the same procedure as that for the SWNT/GC electrode, with exception that the SWNT-OHs were dispersed into ethanol. MB was adsorbed onto bare GC and SWNT-OH/GC electrodes by immersing the electrodes into 1.0×10^{-4} M MB solution for 3 h and the resulting electrodes (denoted as MB/GC and MB−SWNT-OH/GC) were rinsed with water. Electrochemical measurements were carried out with a computer-controlled CHI660A electrochemical analyzer (CHI, Austin, USA) in a conventional and two-compartment cell. Bare and modified GC electrodes were used as a working electrode and a platinum spiral wire as a counter electrode. All potentials were referred to a KCl-saturated Ag/AgCl electrode. A 0.10 M phosphate buffer (pH 7.0) was used as a supporting electrolyte. The electrolyte was deoxygenated by purging pure nitrogen into the solution for about 30 min and nitrogen gas was kept flowing over the solution during the electrochemical

(8) (a) Brown, A. P,; Anson, F. C. *J. Electroanal. Chem.* **1977**, *83*, 203. (b) Katz, E. *J. Electroanal. Chem.* **1994**, *365*, 157. (c) Jaegfeldt, H.; Kuwana, T.; Johansson, G. *J. Am. Chem. Soc.* **1983**, *105*, 1805.

(9) (a) Zhang, J.; Lee, J.-K.; Wu, Y.; Murray, R. W. *Nano Lett.* **2003**, *3*, 403. (b) Li, Q.; Zhang, J.; Hao, Y.; He, M.; Liu, Z. *Carbon* **2004**, *42*, 287. (c) Basiuk, E. V.; Rybak-Akimova, E. V.; Basiuk, V. A.; Acosata-Najarro, D.; Saniger, J. M. *Nano Lett.* **2002**, *1*, 1249. (d) Star, A.; Han, T.; Gabriel, J. P.; Bradley, K.; Gruner, G. *Nano Lett.* **2003**, *3*, 1421.

(10) (a) Borgo, A. C.; Lazarin, A. M.; Gushikem, Y. *Sens. Actuators B* **2002**, *87*, 498. (b) Khoo, S. B.; Chen, F. *Anal. Chem.* **2002**, *74*, 5734. (c) Jain, S.; Dangi, G.; Vardia, J.; Ameta, S. *Int. J. Energy Res.* **1999**, *23*, 71.

(11) Pan, H.; Liu, L.; Guo, Z.; Dai, L.; Zhang, F.; Zhu, D.; Czerw, R.; Carroll, D. L. *Nano Lett.* **2003**, *3*, 29.

measurements. Cyclic voltammetric measurements conducted with the MB−SWNT/GC and MB−SWNT-OH/GC electrodes were subjected to automatic compensation of ohmic potential drop because of the large current recorded.

Layer-by-Layer (LbL) Deposition. MB−SWNT nanostructure was LbL assembled onto an indium tin oxide (ITO)-coated glass plate. The ITO-coated plates were treated by immersing the plates into piranha solution (3:1 v/v concentrated H_2SO_4 and 30% H_2O_2) for 30 min at 50 °C. (*Caution: piranha solution* reacts violently with organics.) After being rinsed with water and dried with N_2, the plates were immersed into a mixed solution of ethanol and 0.1 M NaOH solution with a volume ratio of 6:4 for 2 h. The treated plates were then immersed in a 2 wt % aqueous solution of positively charged PDDA containing 0.5 M NaCl for 30 min to form a positively charged layer of PDDA onto the surface. The PDDA-treated plates were dipped into 2 mg/mL PSS solution for 30 min. After being dried with N_2, the PSS/PDDA-treated ITO plates were immersed into 1.6 mg/mL MB−SWNT solution for 30 min. LbL stepwise assembling of the MB−SWNT/PSS bilayer onto the PDDA-treated ITO plates was conducted by alternately repeating the last two procedures. During each assembling interval, the plates were rinsed with water to remove the excess materials and dried with N_2 bubbling. The formed multilayer nanocompsite was referred to as as $(MB-SWNT/PSS)_n$.

The LbL assembling of the MB−SWNT functional nanostructure into a nanocomposite was characterized by scanning electron microscopy (SEM), ultraviolet−visible−near-infrared spectroscopy (UV−vis−NIR) and electrochemistry. A Quartz slide was used as the substrate to LbL assemble the nanostructure for UV−vis−NIR characterization. The treatment of the quartz slide and the LbL assembling of the (MB−SWNT/PSS) nanocomposite were conducted with the same procedures as those for the ITO plates. For electrochemical characterization, a GC electrode was used for LbL assembling of the $(MB-SWNT/PSS)_n$ multilayer nanostructure with the same procedures as those for the ITO plates. Prior to the assembling, the electrode was first treated at +1.3 V (vs Ag/AgCl) for 10 min in phosphate buffer (pH 7.0) and then coated with a layer of PDDA as described above.

Results and Discussion

Spectroscopic and Electrochemical Evidence for MB Adsorption onto SWNTs. MB is a water-soluble and electroactive polynuclear aromatic dye and its aqueous solution is blue in color. The strong adsorption of MB onto the SWNTs was observed through the large decrease in the UV−vis absorbance of the MB solution upon the dispersion of the SWNTs into the solution (Supporting Information). The adsorption of MB onto the SWNTs to form a MB−SWNT nanostructure was also clearly observed with electrochemistry because of the redox properties of MB. Figure 1 displays cyclic voltammograms (CVs) of the SWNT/GC electrode immersed into MB solution for different times (Panel A). As shown, two pairs of redox waves were observed at −0.15 and −0.26 V. The former wave at −0.15 V was ascribed to the redox process of solution-phase MB at the nanotubes because it mostly disappeared after the electrode was taken out from the MB solution, rinsed with distilled water, and re-cycled in pure phosphate buffer containing no MB as shown in Figure 1 (Panel B). The latter wave at −0.26 V was attributed to the electrochemical process of MB adsorbed on the nanotubes based on the fact that such a redox wave was still clearly recorded when the electrode (MB−SWNT/GC) was re-cycled in the pure phosphate buffer (Figure 1, Panel B). The peak currents at −0.26 V obviously increase with prolonging the time for immersing the electrode into MB solution, suggesting the adsorption and continuous growth of MB onto the SWNTs on GC electrode. This indicates that electroactive MB can adsorb onto the SWNTs, forming an electrochemically functional nanostructure.

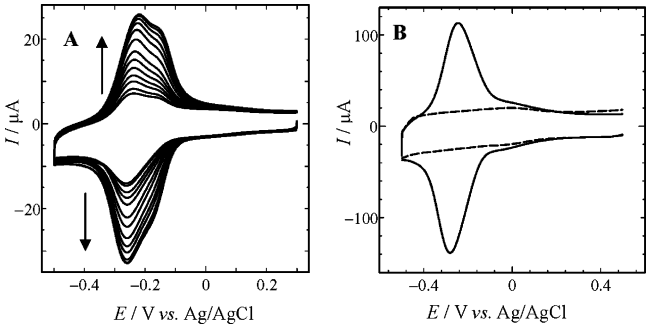

Figure 1. (Panel A)CVs obtained at the SWNT/GC electrode in phosphate buffer containing 1.0×10^{-4} M MB. The electrode was immersed into MB solution for 2, 3, 5, 7, 10, 15, 20, 30, 40, 50, 60, 70, and 80 min (from inner to outer). Scan rate: 50 mV/s. (Panel B) Cyclic voltammograms obtained at the MB−SWNT/GC (solid line) and SWNT/GC (dashed line) electrodes in phosphate buffer. The MB−SWNT/GC electrode was prepared by immersing the SWNT/GC electrode into MB solution for 3 h. Scan rate: 100 mV/s.

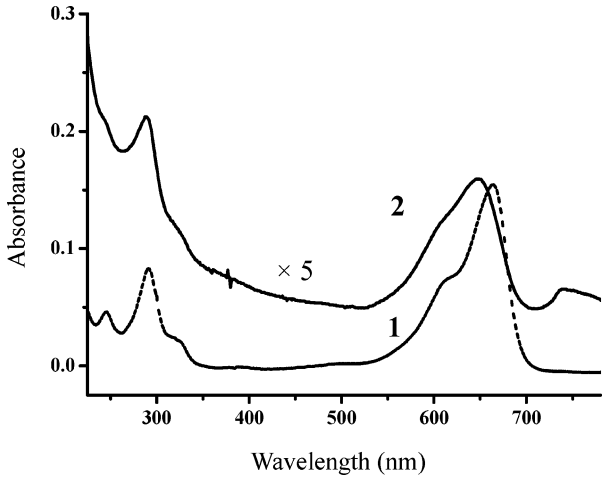

Figure 2. UV spectra of MB (curve 1) and MB−SWNT adsorptive nanostructure (curve 2, with 5× amplification) in water.

Spectroscopic Studies on MB Adsorption onto SWNTs. The formation of a MB−SWNT nanostructure was studied with UV−vis spectroscopy as shown in Figure 2, in which the UV−vis spectra of free MB (curve 1) and the MB−SWNT adduct (curve 2, with a 5× expansion) dispersed in water are displayed. The UV−vis spectrum of the SWNTs dispersed in aqueous solution exhibits a featureless absorption (not shown), whereas the spectrum of free MB in aqueous solution displays a strong absorbance at 663 nm (curve 1), characteristic of the MB monomer in solution. The shoulder at 617 nm was ascribed to the absorbance of the MB dimer in solution.[12] The chemisorption of MB onto the SWNTs was evident from the spectrum of the MB−SWNT adduct (curve 2), which is similar to that of free MB. Moreover, a close inspection of the spectrum of free MB and the

(12) Sagara, T.; Niki, K. *Langmuir* **1993**, *9*, 831.

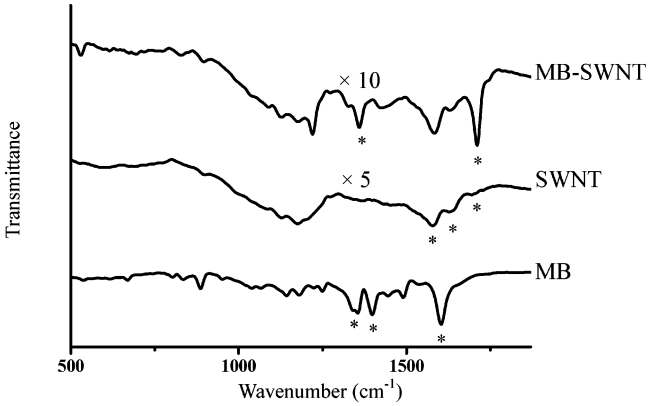

Figure 3. FT-IR spectra of MB (bottom), SWNT (middle, with 5× amplification), and MB−SWNT (top, with 10× amplification).

MB−SWNT adsorptive nanostructure reveals that there is a change in the spectrum of MB after its adsorption onto the SWNTs. For example, two absorption peaks of free MB in solution at 663 and 617 nm were shifted to 646 and 600 nm, respectively, after its adsorption onto the SWNTs. A new peak appeared at 737 nm, which was due to the absorbance of the aggregation of MB molecules onto the SWNTs.[12]

Figure 3 shows the FT-IR spectra of free MB and the MB−SWNT nanostructure. The procedure for SWNT purification is known to produce oxygen-containing moieties, e.g., carboxylic acid groups, at the ends of the nanotubes. The FT-IR spectrum of the purified SWNTs (Figure 3, middle) displays weak bands from 1500 to 1750 cm^{-1} (middle, with 5× amplification). The bands at 1700 and 1630 cm^{-1} were assigned to the C═O stretch mode of carboxylic acid and the stretching mode υ(C═O) of quinone groups produced at the nanotube ends, respectively.[13] The band at 1580 cm^{-1} was attributed to the stretching mode υ(C═C) of double bonds in the nanotube backbone near the functionalized carbon atoms.[13c,14] The FT-IR spectrum of free MB (Figure 3, bottom) exhibits its ring stretch at 1603 cm^{-1}, the symmetric stretch of C−N at 1398 cm^{-1}, and symmetric deformation of $-CH_3$ at 1354 cm^{-1}.[15] Similar to the conclusion drawn from the UV−vis spectra (Figure 2), the adsorption of MB onto the SWNTs was also substantial, based on the FT-IR spectra, since the characteristic spectrum of MB (bottom) was almost recorded in the spectrum of the adsorptive adduct (Figure 3, top, 10× amplification). On the other hand, the FT-IR spectrum of free MB was changed upon its adsorption onto the SWNTs. For instance, the ring stretching band at 1603 cm^{-1} was probably shifted to 1710 cm^{-1} and the symmetric stretch of C−N at 1398 cm^{-1} of MB mostly disappeared after its adsorption onto the SWNTs, implying that this stretch may be largely broadened by the strong interaction between MB and the SWNTs.

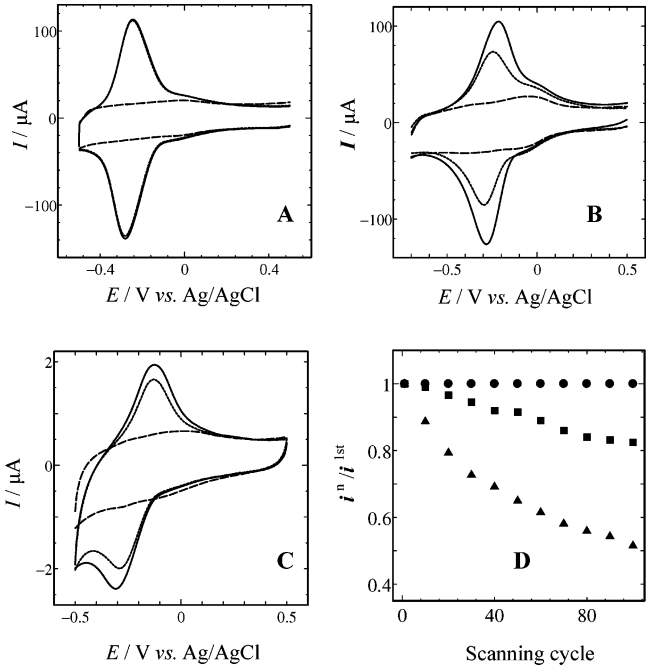

Figure 4. CVs of MB−SWNT/GC (A), MB−SWNT-OH/GC (B), and MB/GC (C) electrodes in phosphate buffer. Dotted and solid curves represent the voltammograms of first and 100th cycles, respectively, and dashed curves represent the voltammograms of the electrodes without MB adsorption. Scan rate, 100 mV/s. (D) The ratio of the cathodic current recorded in successive cycles to the first cycle at the MB−SWNT/GC (●), MB/GC (■), and MB−SWNT-OH/GC (▲) electrodes in phosphate buffer. Scan rate, 100 mV/s.

The above demonstrations further evidence the incorporation of electroactive MB onto the SWNTs, forming an electrochemically functional MB−SWNT nanostructure. Furthermore, the observed changes in the UV−vis and FT-IR spectra that are generally consistent with electron donor−acceptor interaction suggest that a charge-transfer interaction is involved in the structure-associated interactions between MB and the SWNTs. These can be further confirmed by electrochemistry, as demonstrated below.

Electrochemical Studies of MB Adsorption onto SWNTs. The sidewall of the nanotubes is known to mainly consist of sp^2 carbons with a high π-electronic density and a highly hydrophobic property.[16] MB, one of the polynuclear aromatic complexes, may interact with the sidewall of the nanotubes through charge-transfer and hydrophobic interactions. This was demonstrated by comparing the electrochemical properties of MB adsorbed onto various substrates, i.e., GC and SWNT-OHs. Figure 4 compares the typical CVs (1st and 100th cycles) obtained at the MB−SWNT/GC (A), MB−SWNT-OHs/GC (B), and MB/GC (C) electrodes. As reported previously,[11] the sidewall functionalization of covalently bound moieties, i.e., −OH groups in this case, to the SWNT framework essentially and inevitably destroyed the inherent electronic structure of the nanotubes, i.e., changing the sp^2 carbons into sp^3 hybridization, while keeping the tubular structure of the nanotubes. Moreover, such a covalent sidewall functionalization of the nanotubes with −OH groups substantially improved their hydrophilic property. These changes are believed to weaken the interactions (both

(13) (a) Cai, L.; Bahr, J. L.; Yao, Y.; Tour, J. M. *Chem. Mater.* **2002**, *14*, 4253. (b) Mawhinney, D. B.; Yates, J. T., Jr. *Carbon* **2001**, *39*, 1167. (c) Mawhinney, D. B.; Naumenko, V.; Kuznetsova, A.; Yates, J. T., Jr.; Liu, J.; Smalley, R. E. *J. Am. Chem. Soc.* **2000**, *122*, 2383.
(14) Chen, J.; Hamon, M. A.; Hu, H.; Chen, Y.; Rao, A. M.; Eklund, P. C.; Haddon, R. C. *Science* **1998**, *282*, 95.
(15) (a) Imamura, K.; Ikeda, E.; Nagayasu, T.; Sakiyama, T.; Nakanishi, K. *J. Colloid Interface Sci.* **2002**, *245*, 50. (b) Schlereth, D. D.; Karyakin, A. A. *J. Electroanal. Chem.* **1995**, *395*, 221.
(16) Niyogi, S.; Hamom, M. A.; Hu, H.; Zhao, B.; Bhowmik, P.; Sen, R.; Itkis, M. E.; Haddon, R. C. *Acc. Chem. Res.* **2002**, *35*, 1105.

Table 1. Electrochemical Parameters and Stability of the MB-Modified Electrodes

	E_{pa} (V)	E_{pc} (V)	ΔE_p (mV)	$E^{0'}$ (V)	i_{pa}/i_{pc}	$i_{pc}^{100th}/i_{pc}^{1st}$
MB−SWNT/GC	−0.26	−0.27	10	−0.27	0.98	1.00
MB−SWNT-OH/GC	−0.22	−0.28	60	−0.25	1.11	0.52
MB/GC	−0.13	−0.31	180	−0.22	1.15	0.83

electronic and hydrophobic) between MB and the SWNT-OHs. As a consequence, the adsorption of MB onto the SWNT-OHs is anticipated to be weaker than that onto the CNTs, resulting in a poor stability of the MB/SWNT-OH/GC electrode. As expected, we did find that the CV response obtained with such an electrode decreased gradually upon continuous potential cycling as shown in Figure 4B and D. Similarly, the weak interaction between MB and the GC electrode is responsible for the poor stability of the MB/GC electrode (Figure 4C and D). In contrast, the strong interactions of MB with the SWNTs essentially endowed a high stability to the resulting MB/SWNT/GC electrode; for example, the CV response essentially remains identical upon continuously cycling the potential for 100 cycles (Figure 4A and D). Such a high stability is believed to be very useful for practical applications, e.g., electrocatalysis, biosensors, and photovoltaic cells.

As shown in Figure 4B and C, the CVs of the MB adsorbed onto the SWNT-OHs and the GC electrode display a pair of well-defined and broad redox wave, which was attributed to a reversible and irreversible two-electron, one-proton redox process of MB adsorbed on both electrodes in phosphate buffer (pH 7.0).[17] Superior to those, the MB−SWNT/GC electrode shows a pair of mirrorlike and symmetric redox waves with a very small peak separation (ca. 15 mV) and a near unity of the ratio of i_{pa}/i_{pc}, characteristic of the fast electron transfer of MB adsorbed onto the SWNTs. Moreover, a close inspection of the formal potential ($E^{0'}$) of MB in the solution phase (−0.18 V) and adsorbed onto GC, SWNT-OHs, and SWNTs revealed that the $E^{0'}$ was clearly shifted in a negative direction in an order from the solution phase to the adsorbed form from the bare GC, the SWNT-OHs to the SWNTs as summarized in Table 1. The $E^{0'}$ value is known to reflect the electron affinity energetics of electroactive species. While the observed negative shift in the $E^{0'}$ of MB could also possibly stem from the adsorption of MB onto the substrates, we considered that such substantial shift in the $E^{0'}$ of MB onto different substrates in the present case is possibly related to the electron donating or withdrawing character of MB adsorbed onto the SWNTs. This is indicative of charge-transfer interactions between MB and the SWNTs, in which MB may act as an electron acceptor and the SWNT is an electron donor. This is very similar to other kinds of polynuclear aromatic compounds.[9a] Moreover, the differences in the formal potential and the reversibility of MB adsorbed onto a GC and SWNTs essentially suggest that the formed MB−SWNT nanostructure possesses distinct electrochemical properties from MB confined onto a GC electrode as generally used for most electrochemical measurements.

(17) Bard, A. J.; Faulkner, L. R. *Electrochemical Methods: Fundamentals and Applications*; Wiley: New York, 2001.

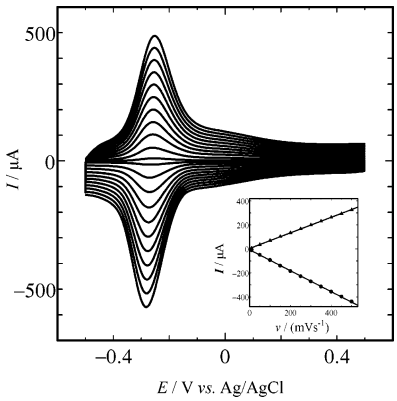

Figure 5. CVs obtained at the MB/SWNT/GC electrode in phosphate buffer. Scan rate (from inner to outer), 10, 50, 100, 150, 200, 250, 300, 350, 400, 450, and 500 mV/s. Inset shows plots of anodic and cathodic peak currents versus potential scan rate.

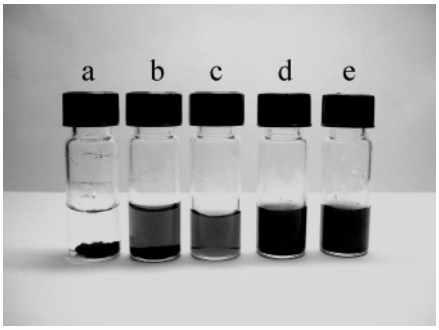

Figure 6. SWNT dispersions in different solutions 2 weeks after ultrasonication. (a) 0.5 mg/mL SWNTs in water, (b) 0.5 mg/mL SWNTs in DMF, (c) 0.1 mg/mL MB−SWNTs in water, (d) 0.5 mg/mL MB−SWNTs in water, and (e) 1.0 mg/mL MB−SWNTs in water.

Figure 5 depicts the cyclic voltammograms of the MB−SWNT/GC electrode in phosphate buffer at various scan rates. As shown, the peak currents are linear with potential scan rates in a range from 10 to 500 mV s^{-1} (inset), while the potential does not change appreciably. This again demonstrates that the redox process of the MB−SWNT nanostructure onto the GC electrode is a fast and surface-confined process.[17]

Solubility and LbL Assembling of the MB−SWNT Nanostructure. Figure 6 compares the solubility of the prepared MB−SWNT nanostructure and the SWNTs. It is known that SWNTs are entangled and are thus relatively difficult to be separated and dispersed in water or organic solvents, i.e., DMF (Figure 6A and B) because of the strong interaction between nanotubes. As can be seen from Figure 6, the adsorption of MB onto the SWNTs essentially solubilizes the formed nanostructure into water (Figure 6C−E) for at least 2 weeks due to the hydrophilicity of the MB molecules and the repellence between positively charged MB molecules adsorbed onto separated nanotubes. In addition to the capability of solubiling the SWNTs in water, the adsorption of MB onto the SWNTs essentially creates a distribution of electronic charges at the tube surfaces which readily facilitated the fabrication of a functional multilayer nanocomposite by the layer-by-layer method, as demonstrated below.

Figure 7 displays typical SEM images of (MB−SWNT/PSS) multilayer films LbL assembled on an ITO wafer.

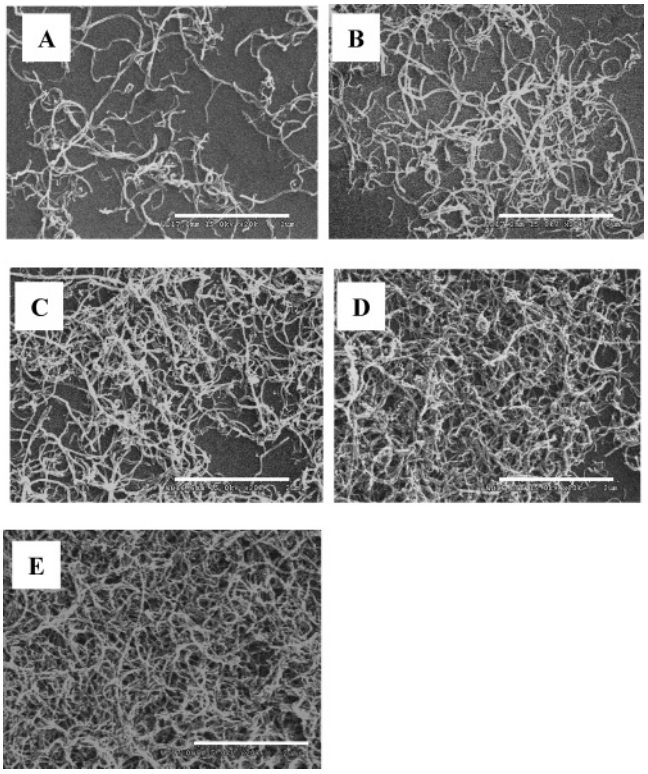

Figure 7. SEM images of $(MB-SWNT/PSS)_n$ films assembled onto PDDA-treated ITO wafer. (A) $n = 1$, (B) $n = 2$, (C) $n = 3$, (D) $n = 4$, and (E) $n = 5$. Scale bar, 2 μm.

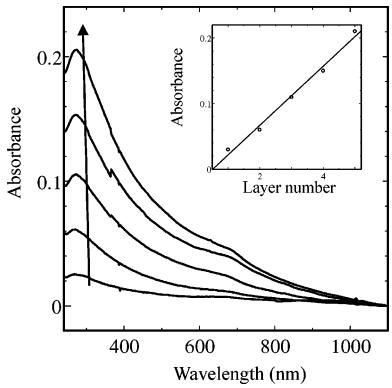

Figure 8. UV−Vis−NIR spectra of $(MB-SWNT/PSS)_n$ multilayer nanostructure assembled onto quartz slide. Inset, absorbance at 270 nm versus the number of the adsorption cycles.

These SEM profiles reveal an obvious increase in nanotube coverage with increasing the number of LBL assembly treatments, indicative of stepwise assembling of the MB−SWNT nanostructure into an electrochemically functional nanocomposite which can be further confirmed by UV−vis−NIR spectroscopy, as shown in Figure 8. PDDA and PSS do not exhibit any absorbance in the wavelength employed, whereas the $(MB-SWNT/PSS)_n$ multilayer films show adsorption at 270 and 680 nm.

The former was characteristic of the absorption of the assembled SWNTs as described previously,[7c−d] while the latter was assigned to the absorption of MB adsorbed onto the SWNTs since such adsorption was not found with the pristine SWNTs. Both absorbances were found to clearly increase with the growth of the films and the amplitude was linear with the layer number (inset in Figure 8). These again confirm the LbL assembling of the nanostructure into a functional nanocomposite with almost the same loading of the MB−SWNT in each layer.

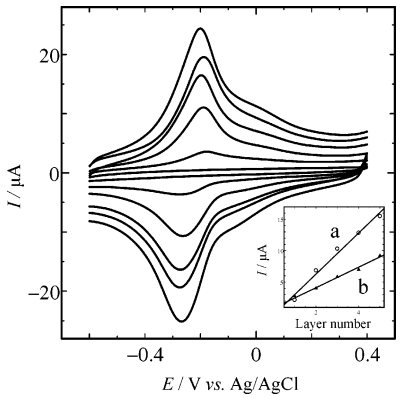

Figure 9. Cyclic voltammograms of the $(MB-SWNT/PSS)_n$ multilayer nanostructure assembled onto GC electrode. Inset plots of anodic Faradaic peak current at −0.20 V (a) and charging current measured at +0.35 V (b) versus the number of the adsorption cycles. Scan rate, 100 mV/s.

The LbL assembling of the prepared nanostructure into an electrochemically functional nanocomposite was further characterized with electrochemistry by virtue of the electrochemical property of MB and the ability of the SWNTs to be used as an electrode material. Figure 9 displays cyclic voltammograms of $(MB-SWNT/PSS)_n$ multilayer films LbL assembled onto GC electrodes. As shown, the layered multilayer films show a pair of well-defined redox peaks at the formal potential of −0.25 V. The currents of these redox peaks clearly increase with increasing the layer number of $(MB-SWNT/PSS)_n$ assembled onto a GC electrode and are linear with the layer number (inset, line A, with cathodic peak current as an example). Moreover, the charging current measured at +0.35 V, which is reflective of the loading of SWNT electrodes onto GC electrode, was also found to be linear with the layer number (inset, line B). These are again indicative of LbL assembling of the nanostructure and the same amount of MB−SWNTs assembled in each layer.

Furthermore, as shown in Figure 4 (Panel A) and Figure 9, the layered $(MB-SWNT/PSS)_n$ nanocomposite possesses almost the same electrochemical properties as MB−SWNT nanostructure, e.g., the same formal potential and the small peak-to-peak separation. This indicates that the nanostructures retain their properties upon layer-by-layer assembly into a functional redox nanocomposite. Moreover, the as-assembled $(MB-SWNT/PSS)_n$ nanocomposite was found to be very stable since the voltammograms obtained for the redox peaks essentially remained identical on continuous potential scanning. The excellent electroactivity and the high stability of the layered nanocomposite are envisaged to make them very useful for basic electrochemical studies and for practical development of electronic devices such as biosensors and photovoltaic cells.

Conclusions

We have demonstrated that MB, a polynuclear aromatic electroactive dye, can stably adsorb onto the SWNTs to form a new type of electrochemically functional MB−SWNT adsorptive nanostructure. Besides the hydrophobic interaction between MB and the SWNTs, UV−visible and IR spectro-

scopic and voltammetric results substantially suggest that there is a charge-transfer interaction between them in which MB is presumably the electron acceptor and the SWNT is the electron donor. The formed MB−SWNT adsorptive nanostructure exhibits good electrochemical properties that are distinct from those of MB adsorbed onto a GC electrode. Furthermore, the adsorption of MB onto the SWNTs is found to solubilize the formed MB−SWNT nanostructure into water and to facilitate layer-by-layer assembling of the prepared electrochemically functional nanostructure into a nanocomposite. The excellent electroactivity and the high stability of the layered nanocomposite are envisaged to make them very useful for basic electrochemical studies and for the development of electronic nanodevices such as biosensors and photovoltaic cells for practical applications.

Acknowledgment. Financial support from National Natural Science Foundation of China (Grant Nos. 20375043 and 20435030 for L.M. and Grant Nos. 50203015, 90306007, 50433020, and 20410019 for Z.G.) and Chinese Academy of Sciences (Grant No. KJCX2-SW-H06 for L.M.) are gratefully acknowledged.

Supporting Information Available: Additional figure (PDF). This material is available free of charge via the Internet at http://pubs.acs.org.

CM0504182